

ARTICLE

Open Access



Potent synergistic efficacy of 2-methoxy-1,4-naphthoquinone derived from quinones against drug-resistant bacteria

Lei Xu^{1†}, Yonglin Zhou^{1,2†}, Deyuan Ou³, Huaizhi Yang¹, Haihua Feng¹, Huangwei Song⁴, Ning Xie⁴, Xiaodi Niu¹, Xuming Deng¹, Meiyang Sun⁵, Peng Zhang⁶, Dejun Liu^{4,7*} and Jianfeng Wang^{1,8*} 

Abstract

The emergence and worldwide dissemination of mobile tigecycline resistance genes *tet(X3)/tet(X4)* posed an enormous threat to the public health. Urgently, feasible strategies must be implemented to restore the clinical efficacy of tetracyclines and prolong the lifespan of existing drugs to address the emerging global antimicrobial resistance threat. Herein, versatile structural scaffolds of quinones for antibiotic adjuvants discovery enlightened a promising and underappreciated reservoir to circumvent the antibiotic resistance. 2-methoxy-1,4-naphthoquinone (MNQ) exhibited the potent potentiation (4 to 32-fold) with tetracyclines, along with effective inhibition on biofilm formation. Mechanistic studies revealed that MNQ synergistically operates with tetracyclines by inhibiting the enzymatic activity of Tet(X3)/Tet(X4) proteins through interaction with their active residues. Furthermore, exposure to MNQ significantly dissipate the proton motive force, leading to a cascade of membrane structural damage and metabolic homeostasis imbalance. Encouragingly, the MNQ-tetracyclines combination showcased substantial therapeutic benefits in two in vivo infection models, as evidenced by the reduced bacterial burden and mitigated pathological injury. Our findings propose a potential therapeutic option and a novel tetracyclines' adjuvant against drug-resistant pathogens carrying Tet(X3)/Tet(X4).

Keywords MNQ, Tetracycline adjuvant, *Tet(X3)/tet(X4)*, Bacterial metabolism

[†]Lei Xu and Yonglin Zhou contributed equally to this work.

*Correspondence:

Dejun Liu

liudejun@cau.edu.cn

Jianfeng Wang

wjf927@jlu.edu.cn

¹ State Key Laboratory for Zoonotic Diseases, Key Laboratory for Zoonosis Research, Ministry of Education, College of Veterinary Medicine, Jilin University, Changchun, China

² Key Laboratory of Ministry of Education for Conservation and Utilization of Special Biological Resources in the Western China, School of Life Sciences, Ningxia University, Yinchuan, China

³ College of Animal Science of Guizhou University, Guiyang, Guizhou, China

⁴ National Key Laboratory of Veterinary Public Health and Safety, College of Veterinary Medicine, China Agricultural University, Beijing, China

⁵ Department of Breast Surgery, Jilin Provincial Cancer Hospital, Changchun, China

⁶ Department of Thoracic Surgery, The First Hospital of Jilin University, Changchun, China

⁷ College of Veterinary Medicine, China Agricultural University, Beijing, China

⁸ College of Veterinary Medicine, Jilin University, Changchun, China



Introduction

Over the past 100 years [1], antibiotics were broadly used in bacterial infection therapeutics and drastically changed modern medicine. Since 1980s, a gradual decline in antibiotics discovery and the development of multidrug resistance have led to a surge of drug-resistant bacterial infections and seriously threatened the therapeutic options, with a potentially estimated 700,000 deaths attributed to antimicrobial resistance (AMR) annually [2]. Urgently, alternative strategies to tackle the crisis were absolutely imperative.

Alarmingly, with the emergence of metallo- β -lactamases (MBLs)-mediated carbapenems resistance [3] and MCR-mediated colistin-resistance [4], tigecycline was conferred as a last-resort antibiotic to address serious infections. Nevertheless, the potency of tetracyclines is compromised by multiple resistance mechanisms, including acquirement of catalyzing enzyme, overexpression of multidrug efflux pumps, bacterial membrane permeability changes and alteration of target sites [5, 6]. Notably, recent investigations implied that the evolution of transferable high-level tetracyclines resistance by the novel *tet(X)* orthologs confers an enormous threat to the efficacy of next-generation tetracyclines (tigecycline, omadacycline, and eravacycline) [7]. The emergence of novel plasmid-mediated tigecycline resistance genes *tet(X3)/tet(X4)* in Enterobacteriaceae constitutes a serious threat for therapeutic options and public health [8]. Additionally, more than 30 tetracycline-specific efflux pump genes and nine MDR efflux pump genes of the resistance-nodulation-cell division (RND) family have been found to impair tetracyclines susceptibility [9]. Scientifically, focusing on these resistant mechanisms is the most effective and feasible strategy to prolong the lifespan of conventional antibiotics and tackle the crisis of antibiotic resistances.

It is an emerging model of antibiotic-mediated death in bacteria involving dysregulation of central metabolism and energetic pathways [10]. Accumulating evidences support the involvement of multifarious bacterial metabolic pathway, for instance, the tricarboxylic acid (TCA) cycle and oxidative phosphorylation (OxPhos) pathway, thereby inducing in bacterial death [11]. Hence, the metabolic reprogramming might be a novel promising strategy for the development of antibiotic adjuvants.

To date, the progress of novel antibiotics discovery was lagging far behind the rapid dissemination of MDR pathogens globally. Therefore, extending the antibiotic adjuvants and the combination therapy exhibited tremendous potential for infection therapeutics [12]. Given that previous studies found the potentiation potency of plumbagin with tetracyclines [13], we further explored the potential mechanisms underlying the synergistic effects of quinones. In the current study,

2-methoxy-1,4-naphthoquinone (MNQ) with negligible cytotoxicity displayed potentiation activity with tetracyclines in Tet(X3)/Tet(X4)-producing pathogens in vivo/in vitro. Collectively, our study confirms that MNQ is a promising candidate for the development of 1,4-naphthoquinones as a novel and safe tetracyclines adjuvant. Our discovery provided an effective therapeutic regimen for combating MDR pathogens infections and the distinctive mechanisms displayed potent promise for the drug discovery and development.

Results

Screening of quinones-tetracyclines combinations identify MNQ and tetracyclines synergism against Tet(X3)/Tet(X4)-producing *E. coli*

To date, numerous quinone-derived compounds have attracted increasing interests due to the abundant biological activities, such as antimalarial [14], antidiabetic [15], anti-inflammatory [16], and antibacterial [17] potentials. The emergence of resistance to the last-resort antibiotic tigecycline (due to large scale use) and therapeutic failure are the alarming obstacles to combat MDR pathogens infections globally [8]. Nowadays, an adjuvant therapy could become an effective first-line-treatment strategy against MDR pathogens until new antibacterial drugs are available. Our recent evidence has emerged indicating that plumbagin, as a natural naphthoquinone, was identified as a potent broad-spectrum inhibitor of Tet(X3)/Tet(X4) with the antibacterial synergistic activity plus tetracyclines [13]. Hence, the largely unexplored novel property of quinones, remains an intriguing potential target against multiple drug-resistant bacterial infections.

Quinones, as a key source for future medicine development, are ubiquitous in nature and formed through diverse mechanisms [14]. Notably, 1,4-Naphthoquinone (1,4-NQ), a class of natural compounds derived from naphthalene, contain a 1,4-naphthalenoid ring and easily susceptible to reduction, oxidation, and addition or substitutions of one or more methyl, hydroxyl and/or methoxy. Together, the high reactivity and the mature chemical modification technology of quinones make these natural products potential for the profound development of novel types of substances with abundant biochemical properties, and provide new targets and strategies for addressing multiple challenges.

Therefore, 28 widely used quinones, as listed in Supplementary Table 3, were screened using antimicrobial susceptibilities assay (Fig. 1a). Dramatically, plumbagin, 2-methoxy-1,4-naphthoquinone (MNQ), 2,3-dichloro-1,4-naphthoquinone (DNQ) and p-benzoquinone restored the susceptibility of tetracyclines (including tetracycline and tigecycline) against *tet(X4)*-positive bacteria (Supplementary

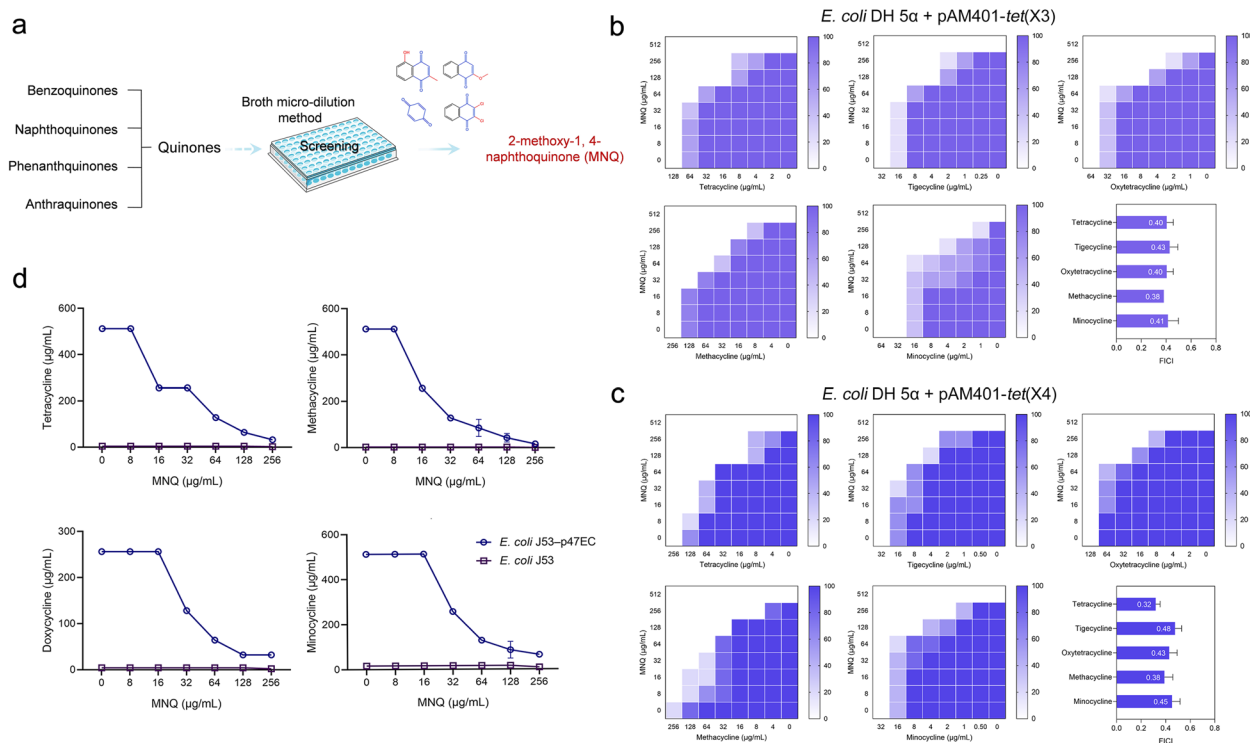


Fig. 1 MNQ extensively potentiates tetracyclines activity. **a** The screening scheme of candidate compounds in the current study. The effective synergists against *tet(X4)*-positive *E. coli* were derived from 28 quinones using the broth micro-dilution method. **b–c** MNQ effectively synergized with tetracycline antibiotics (including tetracycline, tigecycline, oxytetracycline, methacycline, minocycline) against *E. coli* DH5α + pAM401-*tet(X3)* (**b**) and *E. coli* DH5α + pAM401-*tet(X4)* (**c**) by chequerboard broth microdilution assays. Dark regions represent higher cell density. **d** MNQ restored the susceptibility of multiple tetracyclines against *tet(X4)*-carrying *E. coli* J53p47EC. The experiments were repeated at least three times independently. FIC index ≤ 0.50 was defined as synergism

Table 3). The results suggested that compounds which contain the cyclohexadienedione structure exhibited a distinct activity range depending on the electronic nature of different active fragments and their various substituents. Remarkably, MNQ along with high potency, selectivity and negligible toxicity manifested a broad-spectrum synergistic activity against drug-resistant bacteria harboring Tet(X3)/Tet(X4) (Fig. 1b and c), which could be explored as a potential tetracyclines synergist with a novel mechanism of action. Taken together, MNQ was selected as a representative to analyse the mechanisms underlying the recovery of bacterial sensitivity to tetracycline antibiotics.

MNQ is an effective broad-spectrum synergist

To further test the potentiation, we assessed the synergistic effects against *tet(X)*-positive clinical isolates, such as *E. coli* 47EC, *A. baumannii* 34AB and various *tet(X4)*/*tet(X6)*-positive isolates. Notably, MNQ administration effectively restored the sensitivity of tetracyclines against *tet(X)*-positive clinical isolates (Supplementary

Fig. 1a–d; Supplementary Tables 4 and 5). Further, *E. coli* J53 and *K. pneumoniae* K12016 were successfully conjugated *tet(X4)*-carrying p47EC to obtain the resistance [8]. In the presence of MNQ, the antibacterial efficacy of tetracyclines against *tet(X4)*-carrying *E. coli* J53p47EC and *K. pneumoniae* K12016p47EC observably boosted (Fig. 1d; Supplementary Fig. 1e).

To demonstrate the broad-spectrum synergistic effect of MNQ, we additionally evaluated the potency of the combination of MNQ with various antibiotics using chequerboard microdilution assays. Interestingly, MNQ at sub-MIC levels potentiated multiple antibiotics activity, such as lincomycin and erythromycin, against diverse Tet(X3)/Tet(X4)-producing pathogens infections (Supplementary Fig. 2), suggesting that MNQ plus multiple antibiotics, especially tetracyclines, is a potential antibacterial and anti-infection strategy against bacterial infections. These findings demonstrated that MNQ was a promising broad-spectrum antibiotics adjuvant for fighting MDR bacteria infections.

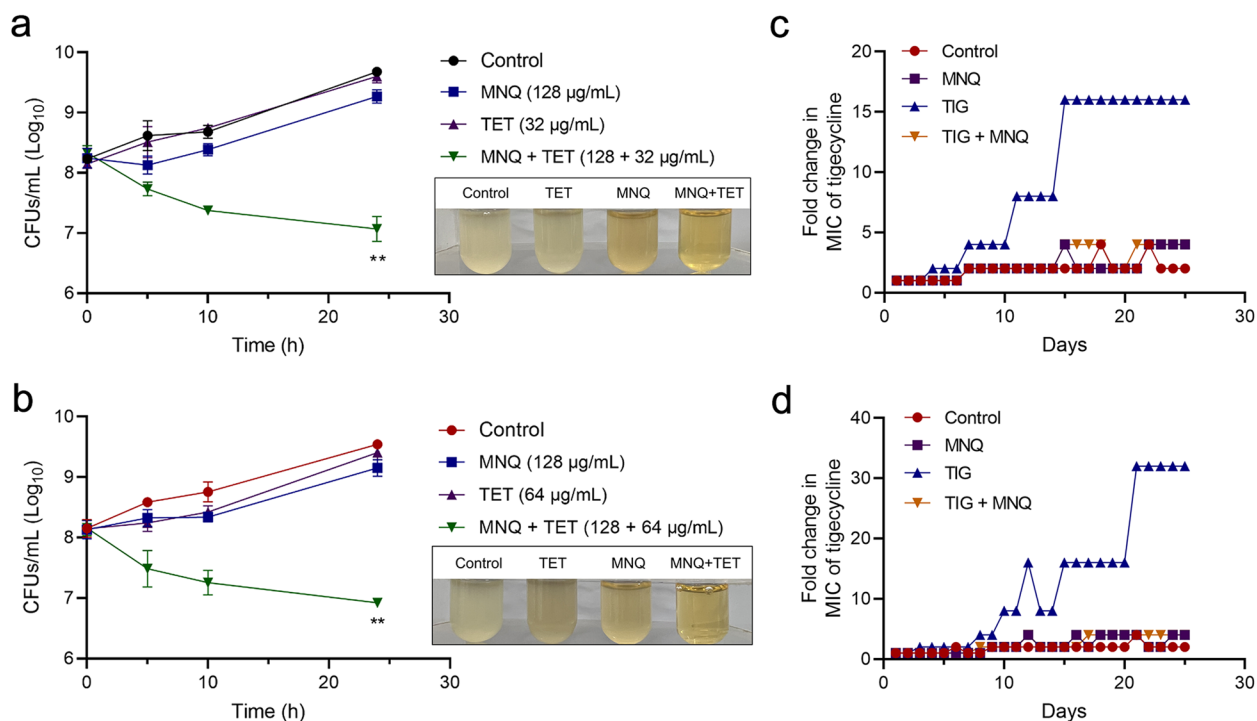


Fig. 2 MNQ enhances tetracyclines efficacy and thwarts the emergence of resistance. Time-dependent killing curves of MNQ combined with tetracycline (TET) against *E. coli* DH5α + pAM401-*tet*(X3) (a) and *E. coli* DH5α + pAM401-*tet*(X4) (b). And emergence of tigecycline resistance in *E. coli* DH5α + pAM401-*tet*(X3) (c) and *E. coli* DH5α + pAM401-*tet*(X4) (d) during 25 serial passages in the absence or presence of sub-MIC levels of MNQ, TIG or the combinations. The experiments were repeated three times independently, and the representative data were shown. ***P* < 0.01

To further illustrate the potentiation of MNQ plus tetracyclines, the time-killing assay were performed to investigate their synergistic bactericidal activity. Excitingly, the combination of MNQ plus tetracycline (Fig. 2a and b) exhibited potent synergistic effects against *E. coli* DH 5α + pAM401-*tet*(X3)/*tet*(X4), despite difficult to abrogate exponentially growing cells thoroughly.

To explore the ability of MNQ on the evolution of tigecycline resistance, serial passages of *tet*(X3)/*tet*(X4)-positive *E. coli* supplementing with tigecycline in the presence and absence of MNQ for 25 days were performed. Excitingly, MNQ co-administrated with tigecycline significantly suppressed the evolution of tigecycline resistance (Fig. 2c and d). By contrast, MIC values of tigecycline treatment group were increased by 16-fold (*E. coli* DH 5α + pAM401-*tet*(X3)) and 32-fold (*E. coli* DH 5α + pAM401-*tet*(X4)) (Fig. 2c and d). These findings suggested that combined therapy with MNQ could hardly bring the selective pressure for the evolution of resistance.

MNQ in combination with tetracycline impairs biofilm formation and maturation

Biofilms play an important role in the bacterial survival, colonization and pathogenesis [18]. Therefore, biofilm

formation and inhibition assays were further employed to probe the efficacy of MNQ on the inhibition of the bacterial biofilms formation. As indicated in Fig. 3a and b, MNQ treatment showed a significant inhibition on biofilm formation of *E. coli* DH 5α + pAM401-*tet*(X4) and a decreased biomass compared to the untreated control group. Moreover, the inhibitory effect on the development of *E. coli* DH 5α + pAM401-*tet*(X4) biofilms were also observed while MNQ in combination with tetracycline (Fig. 3a and b). Consistently, confocal laser scanning microscope images showed that MNQ monotherapy, or in combination with tetracycline resulted in a thinner and structurally incomplete layer of cells (Fig. 3c). Additionally, the combinations effectively decreased the biofilm formation of *E. coli* DH 5α + pAM401-*tet*(X3) (Supplementary Fig. 3a).

We further investigated whether MNQ also contributed to the disruption of pre-existing biofilm structures. As depicted in Fig. 3d and e, with the addition of MNQ, or the combinations with tetracycline to the developing *E. coli* biofilms, the biofilms development and maturation were significantly inhibited, as evidenced by a decreased crystal violet (CV) quantification and bacterial biomass. Consistent with these results, a rare density of attached biomass and fragmentary biofilm were observed in the

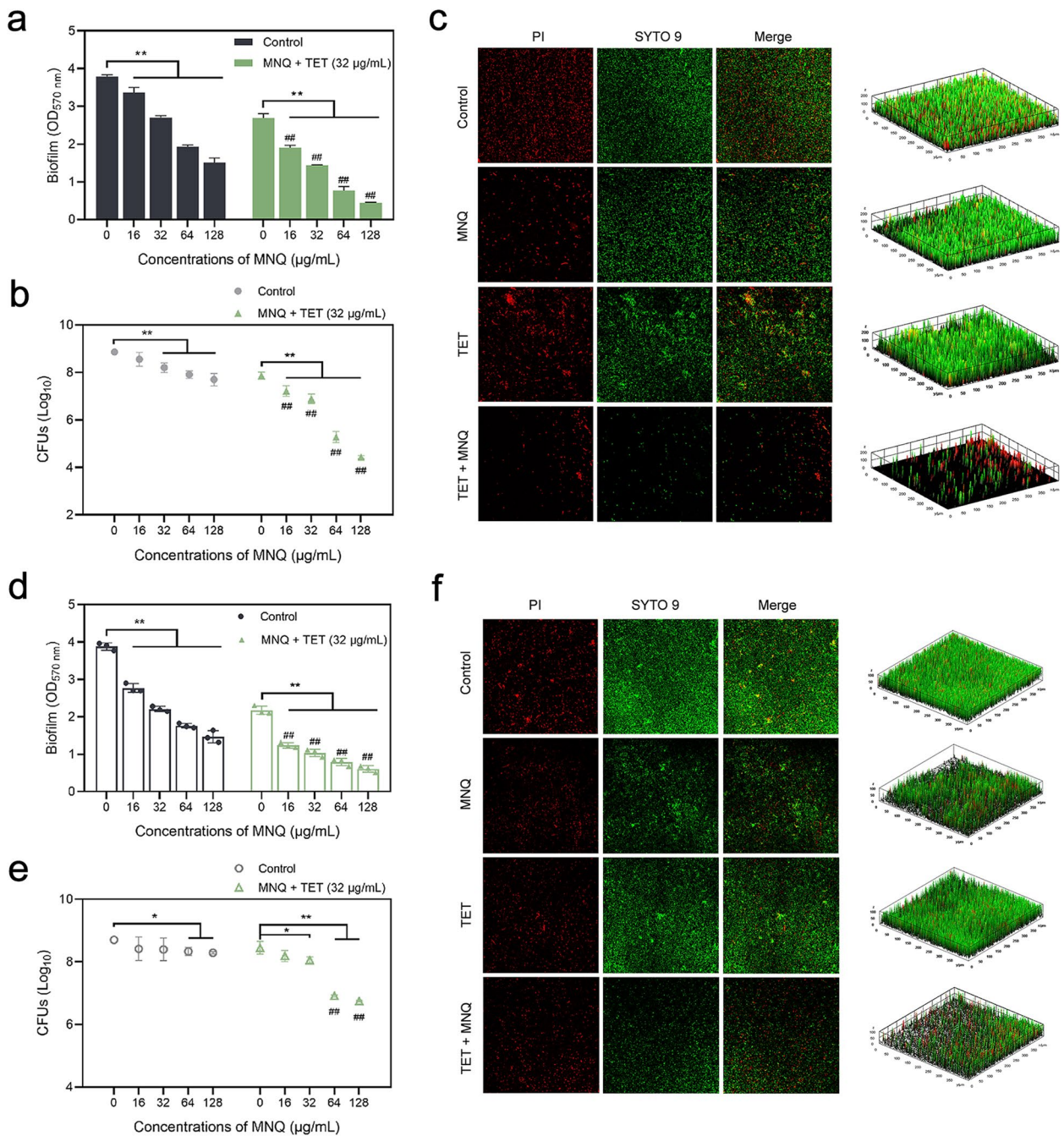


Fig. 3 Effect of MNQ, or in combination with tetracycline on the biofilm formation and maturation. *E. coli* DH5 α +pAM401-*tet*(X4) biofilms were grown for 24 h with the presence or absence of MNQ and/or tetracycline (TET) (a–c). Additionally, the indicated concentrations of MNQ and/or TET were subsequently added at 12 h post-inoculation for an additional 12 h-incubation to assess the disruption of preformed *E. coli* biofilms by MNQ or the combinations (d–f). The graphs presented the OD_{570 nm} values of crystal violet (CV)-staining biofilms (a, d) and biomass (CFUs) quantified by the microbiological plating (b, e). c, f Confocal microscopy images of *E. coli* biofilms grown with or without MNQ and/or TET. Fluorescence intensity of each sample represents biofilms thickness. The representative image was chosen from three independent replicates. All data were repeated three times independently. ***P* < 0.01 and **P* < 0.05 vs. the control group; ##*P* < 0.01 vs. MNQ monotherapy group

MNQ monotherapy and MNQ+TET groups (Fig. 3f), suggesting that MNQ addition could disrupt the development of biofilm and deactivate bacteria. Such inhibitions were also observed in the biofilms maturation against *E.*

coli DH 5 α +pAM401-*tet*(X3) (Supplementary Fig. 3b). Collectively, these observations concluded that MNQ works synergistically with tetracycline to impair the biofilms formation and maturation, which underscored the

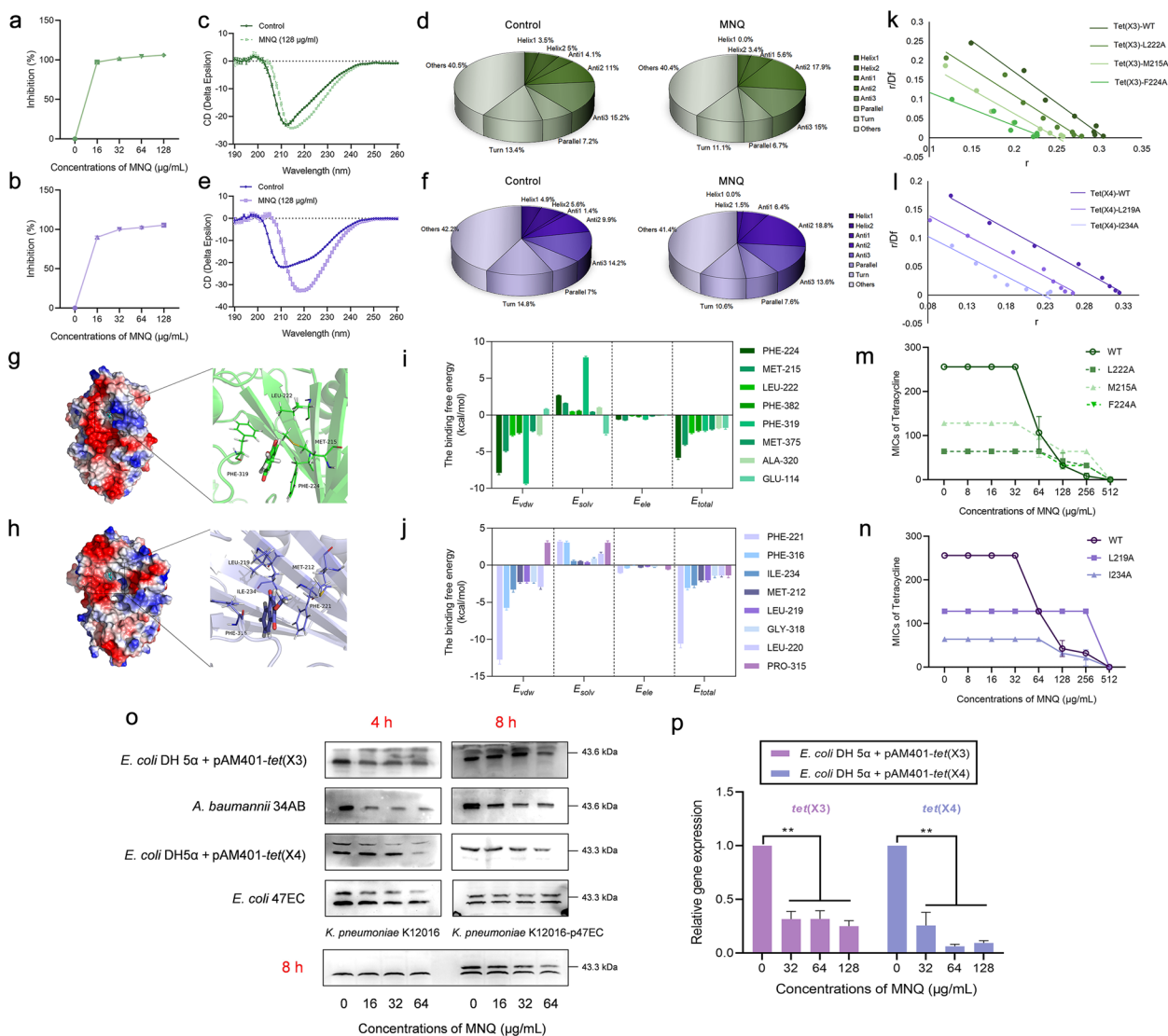


Fig. 4 Molecular mechanisms of MNQ interacting with Tet(X3)/Tet(X4). The catalytic activity of Tet(X3) (a) and Tet(X4) (b) following the diverse concentrations of MNQ incubation. The circular dichroism (CD) spectroscopy analysis of Tet(X3) (c–d) and Tet(X4) (e–f) treated with DMSO or 128 µg/mL MNQ. The binding mode of MNQ/Tet(X3) complex (g) or MNQ/Tet(X4) complex (h) obtained from molecular docking simulations. Decomposition of the binding energy (including E_{vdw} , E_{elec} , E_{solv} and E_{total}) on the binding residues between MNQ and Tet(X3) (i) or Tet(X4) (j). The binding constants of MNQ engaging with Tet(X3)-WT and the mutants (k), Tet(X4)-WT and the mutants (l). m–n The synergistic activity of MNQ against Tet(X3)/Tet(X4)-mutated stains at the indicated binding sites was determined by broth micro-dilution methods. o Tet(X3)/Tet(X4) levels in the precipitates of bacterial cultures treated with or without MNQ were assessed by western blotting. p The mRNA levels of *tet(X3)/tet(X4)* in the *E. coli* DH5α + pAM401-*tet(X3)/tet(X4)* were quantified by real-time PCR and normalized to 16S rRNA. The data are representative of three biological replicates and expressed as ± SEM. ** $P < 0.01$

therapeutic potential of MNQ against drug-resistant pathogens infections.

Determination of the interaction between MNQ and Tet(X3)/Tet(X4)

Considerable evidence revealed that Tet(X3)/Tet(X4) are tetracycline-inactivating monooxygenase, the presence of which severely compromises the efficacy of tetracyclines.

And the catalytic activity of Tet(X3)/Tet(X4) could be evaluated by monitoring the changes in absorbance values at 400 nm [19]. Accordingly, as shown in Fig. 4a and b, MNQ exhibited an obvious inhibitory efficacy on the catalytic activity of Tet(X3)/Tet(X4), suggesting that MNQ represents an effective Tet(X3)/Tet(X4) inhibitor that reverses tetracyclines activity against *tet(X3)/tet(X4)*-positive pathogens. To initially explore the molecular

basis for the suppression of Tet(X3)/Tet(X4) activity by MNQ, the secondary structures of Tet(X3)/Tet(X4) supplemented with or without MNQ were determined using a CD spectroscopy analysis. Dramatically, co-administrated with MNQ resulted in obvious alterations in the secondary structures of Tet(X3) (Fig. 4c and d) and Tet(X4) (Fig. 4e and f), as evidenced by significant decrease in α -helix1, α -helix2 and turn conformations and increase in anti-1 and anti-2 conformations (Fig. 4c and f), suggesting that a direct engagement of MNQ with Tet(X3)/Tet(X4) accompanying the alternation of second structure may contribute to the inhibitory potent of MNQ.

The potential binding mode between MNQ and Tet(X3)/Tet(X4) was further determined using molecular docking and molecular dynamics (MD) simulations. Initially, the root-mean-square deviation (RMSD) value of the complex was calculated for the subsequent MD simulations. As revealed, MNQ could localize to the catalytic pocket of Tet(X3)/Tet(X4) and the active residues of Tet(X3) (LEU222, PHE319, PHE224 and MET215) and Tet(X4) (LEU219, MET212, ILE234, PHE221 and PHE316) could form strong interactions with MNQ as shown in the binding modes (Fig. 4g and h). Specifically, the residues and their contribution to the system were calculated using the MM-PBSA approach. As indicated in Fig. 4i, PHE224 and PHE319 of Tet(X3) with a E_{vdw} of less than -5 kcal/mol, which showed a strong *van der Waals* interaction with MNQ. Similarly, PHE224 and PHE319 were observed to exhibit prominent solvation contribution ($E_{solv} \geq 1.0$ kcal/mol). Additionally, the residues PHE221, PHE316 and ILE234 of Tet(X4) also exhibited appreciable *van der Waals* interactions with MNQ (Fig. 4j).

On the basis of above results, site-specific mutagenesis and fluorescence quenching assays were further performed to confirm the binding mode of MNQ and Tet(X3)/Tet(X4). As expected, the binding constants for the interaction between MNQ and Tet(X3)/Tet(X4) mutants were significantly decreased (Fig. 4k and l), suggesting that the binding of Tet(X3)/Tet(X4)-WT with MNQ is evidently stronger than mutants. As shown in Fig. 4m and n, the mutants were more sensitive to tetracycline in comparison with the Tet(X3)/Tet(X4)-WT and the synergistic effects of MNQ combined with tetracycline against the mutants were significantly decreased compared to the wild-type *E. coli* DH5 α -pGEX-4 T-1-Tet(X3)/Tet(X4). Collectively, these results suggested that MNQ is a potent Tet(X3)/Tet(X4) inhibitor by occupying residues L222, M215, F224 of Tet(X3) and L219, I234 of Tet(X4).

We further tested whether MNQ affects the expression of Tet(X3)/Tet(X4). As shown in Fig. 4o, MNQ treatment displayed a significant inhibition on the expression

of Tet(X3)/Tet(X4), in both transformants (*E. coli* DH5 α +pAM401-*tet*(X3) and *E. coli* DH5 α +pAM401-*tet*(X4)) and the isolates (*E. coli* 47EC and *A. baumannii* 34AB). Consistently, MNQ-mediated inhibition of Tet(X3)/Tet(X4) production was observed in *tet*(X4)-carrying *K. pneumoniae* K12016-p47EC; Nevertheless, not in the wide-type recipient tigecycline-susceptible *K. pneumoniae* K12016 strain (Fig. 4o). Further exploration indicated that the transcription of resistance gene *tet*(X3)/*tet*(X4) in *E. coli* exhibited prominent inhibition effect by MNQ (Fig. 4p). These results together demonstrated that MNQ potentially inhibited the catalytic activity and production of Tet(X3)/Tet(X4) by engaging with the catalytic pocket of Tet(X3)/Tet(X4).

Mechanisms of the synergy of MNQ with tetracyclines

Given the broad-spectrum potentiation of MNQ to multiple antibiotics, we next sought to explore the potential synergistic mechanisms. Considerable evidences revealed that bacterial resistance might be associated with an increase of intracellular reactive oxidative species (ROS), which in turn, could potentially undermine the membrane integrity [20]. We therefore inferred that MNQ, in combination with tetracyclines, might destruct the cell membrane integrity. As shown in Fig. 5a, addition of MNQ combined with tetracycline to *tet*(X4)-positive *E. coli* led obvious swelling or wrinkling on the surface of bacteria and eventual lysis of cells, while monotreatment exhibited insignificant effects on the bacterial morphological damage. These results indicated that MNQ could potentially restore the antimicrobial effect of tetracyclines by triggering membrane damage. Further, the antimicrobial activity of MNQ in combination with tetracycline was further confirmed using the LIVE/DEAD BacLight viability assay, as shown by increased numbers of PI-labeled dead bacteria (red fluorescence) by combination treatment, whereas relatively weaker red fluorescence and stronger green fluorescence were observed by the monotreatment in both *tet*(X3)/*tet*(X4)-positive *E. coli* (Fig. 5b and c; Supplementary Fig. 4a and b). Furthermore, We assessed the membrane permeability using a fluorescent probe propidium iodide (PI). The data revealed that membrane permeability was dramatically increased by the addition of MNQ, confirmed by an enhanced fluorescence intensity (Fig. 5d and e), agreeing with the bacterial viability observation. Collectively, these results suggested that MNQ manifested an obvious impact on the inner membrane permeability.

Considerable evidences revealed that bacterial membrane damage was closely relevant to the proton motive force (PMF) required for ATP synthesis, which is a form of potential energy consisting of $\Delta\psi$ (membrane potential) and ΔpH (proton gradient) [21]. As observed in

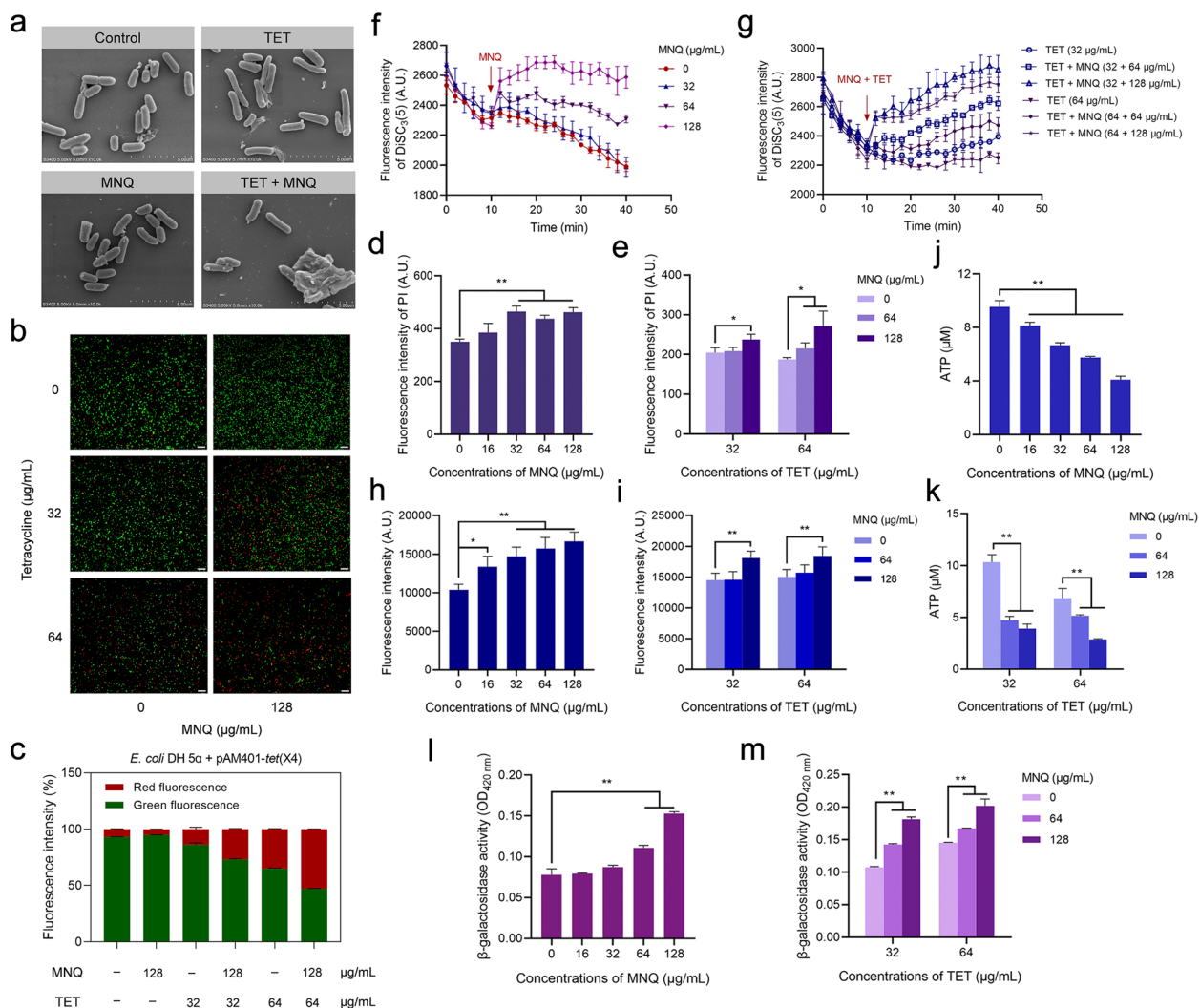


Fig. 5 Synergistic mechanisms of MNQ-tetracyclines combination. **a** MNQ, or in combination with tetracycline (TET) triggered membrane damage, as evidenced by SEM observation. **b** *E. coli* DH5 α + pAM401-*tet*(X4) cells treated with or without MNQ and/or TET. Live cells were stained green by SYTO9 and dead cells were stained red by PI. **c** Further, percentages of live/dead cells present in each samples were quantified using ImageJ software. **d-e** Increased membrane permeability of propidium iodide (PI)-labeled *E. coli* cells with the addition of MNQ. MNQ (**f**) or in combination with TET (**g**) dissipated membrane potential of *E. coli* DH5 α + pAM401-*tet*(X4). The drugs were supplemented into the cultures following DiSC₃(5) dye incubation for 10 min, and the fluorescence intensity was continuously monitored for additional 30 min. **h-i** The effect of MNQ or the combinations on intracellular Δ pH was determined using fluorescence dye BCECF-AM-probed *E. coli* cells. **j-k** Accordingly, decreased level of ATP production in *E. coli* cells were exhibited in a MNQ-dependent manner. **l-m** β -galactosidase activity in the culture media of *E. coli* with the presence or absence of MNQ and/or tetracycline. All data were repeated three times independently, and the representative data were shown. ** $P < 0.01$; * $P < 0.05$

Fig. 5f–i, MNQ administration dissipated the proton motive force (PMF), as evidenced by the disruption of $\Delta\psi$ (membrane potential; Fig. 5f and g) and Δ pH (proton gradient; Fig. 5h and i). Because PMF directly drives ATP production, the intracellular ATP was sequentially decreased by the co-administrated with MNQ (Fig. 5j and k). Cumulatively, with the membrane permeability increasing, the monotherapy with MNQ or combination therapy resulted in a notably increased levels of cellular

contents, such as β -galactosidase (Fig. 5l and m). These results indicated that MNQ triggered membranes damage by the disruption of proton motive force.

Microbes encode a diverse range of multidrug transporters, most of which are rely on the proton motive force (PMF) [21]. We further evaluated the efflux activity of bacteria using rhodamine as an indicator, as expected, exposure to MNQ markedly decreased the efflux of rhodamine in *tet*(X4)-positive *E. coli* (Fig. 6a and b).

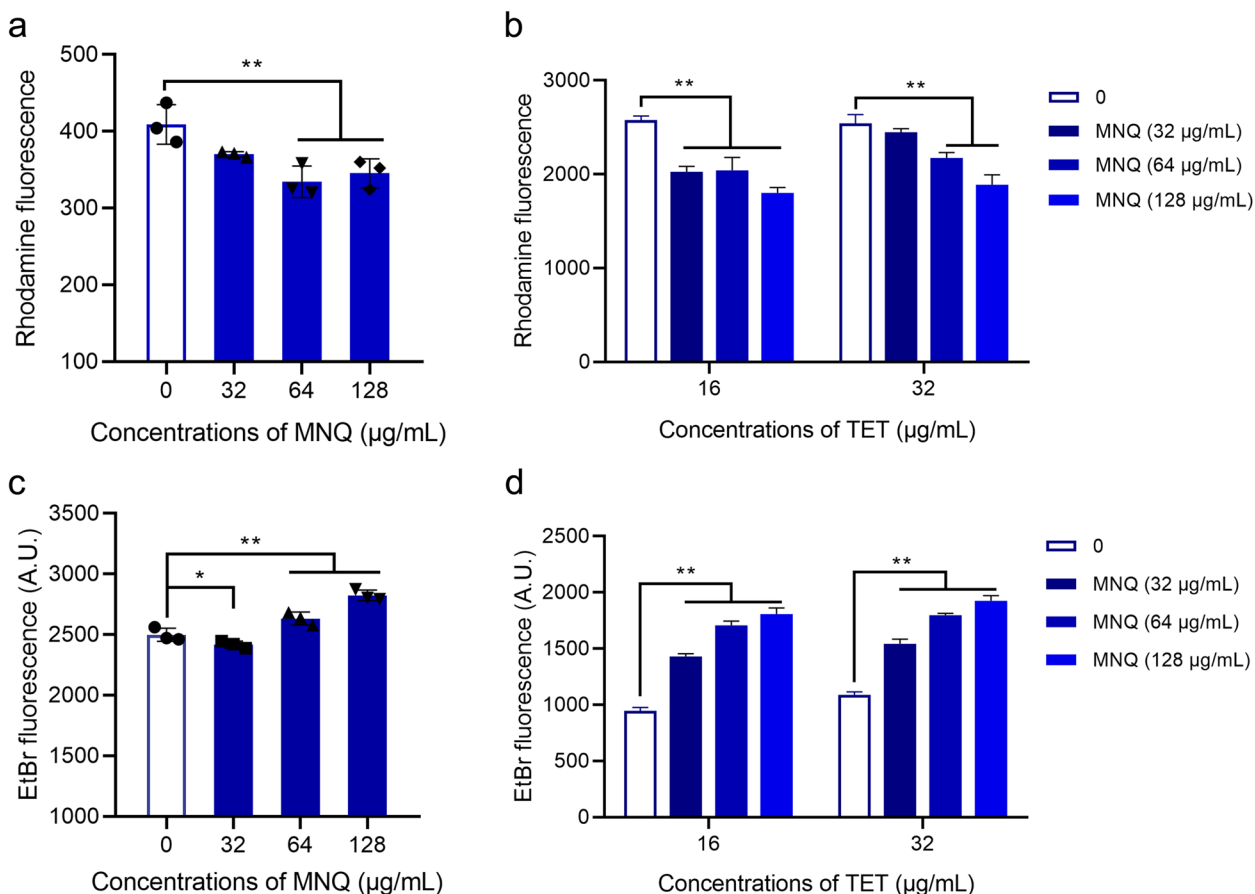


Fig. 6 MNQ deprives the function of multidrug-resistant efflux pumps. Efflux pump activities of *E. coli* DH5a + pAM401-*tet*(X4) with the treatment of MNQ or in combination with tetracycline were determined using the fluorescence dye Rhodamine (a–b) or Ethidium bromide (EtBr) (c–d). All data were repeated three times independently. ** $P < 0.01$; * $P < 0.05$

Furthermore, to quantify the inhibition effect of MNQ on the efflux activity, the ethidium bromide (EtBr) efflux in *E. coli* cells were suppressed by the MNQ treatment. Collectively, overall results indicated that MNQ potentiated antibiotics activity, attributing to the destruction of bacterial PMF and the inhibition of efflux pumps efficacy.

Multivariate data analysis of bacterial metabolites

Metabolomics was employed to further analyse the effect of MNQ on the bacterial metabolic homeostasis. As for the PCA model, the scatter points were distinctly separated between the control and MNQ treatment groups in the NEG mode (Supplementary Fig. 5a) and POS mode (Supplementary Fig. 5b). Further, the OPLS-DA model was established to distinguish the differential metabolites between the two groups (Supplementary Fig. 5c–f). Specifically, the R2Y and Q2 were 0.996 and 0.908 in the NEG mode and 0.991 and 0.81 in the POS mode, respectively (Supplementary Fig. 5e and f). As shown in Fig. 7a and b, differentially enriched

metabolites were identified and the heat maps analysis indicated that 114 metabolites were down-regulated and 83 metabolites were up-regulated in the NEG mode and moreover, 62 metabolites were down-regulated and 92 metabolites were up-regulated in the POS mode. Furthermore, KEGG and MetaboAnalyst analysis were employed to identify the significantly enriched metabolic pathways. As indicated in Fig. 7c and e, purine metabolism, TCA cycle, arginine biosynthesis, and alanine, aspartate and glutamate metabolism exhibited significant difference ($P < 0.05$) in the NEG mode. And beta-alanine metabolism, *E. coli* biofilm formation and ATP-binding cassette (ABC) transporter pathway were prominently enriched in the POS mode (Fig. 7d and f). Collectively, bacterial metabolites differences indicated that MNQ addition significantly interfered with bacterial metabolism, which prompts us to focus on the above mentioned pathways. And an imbalance in metabolic homeostasis induced by MNQ might eventually lead to an advancement in cell death.

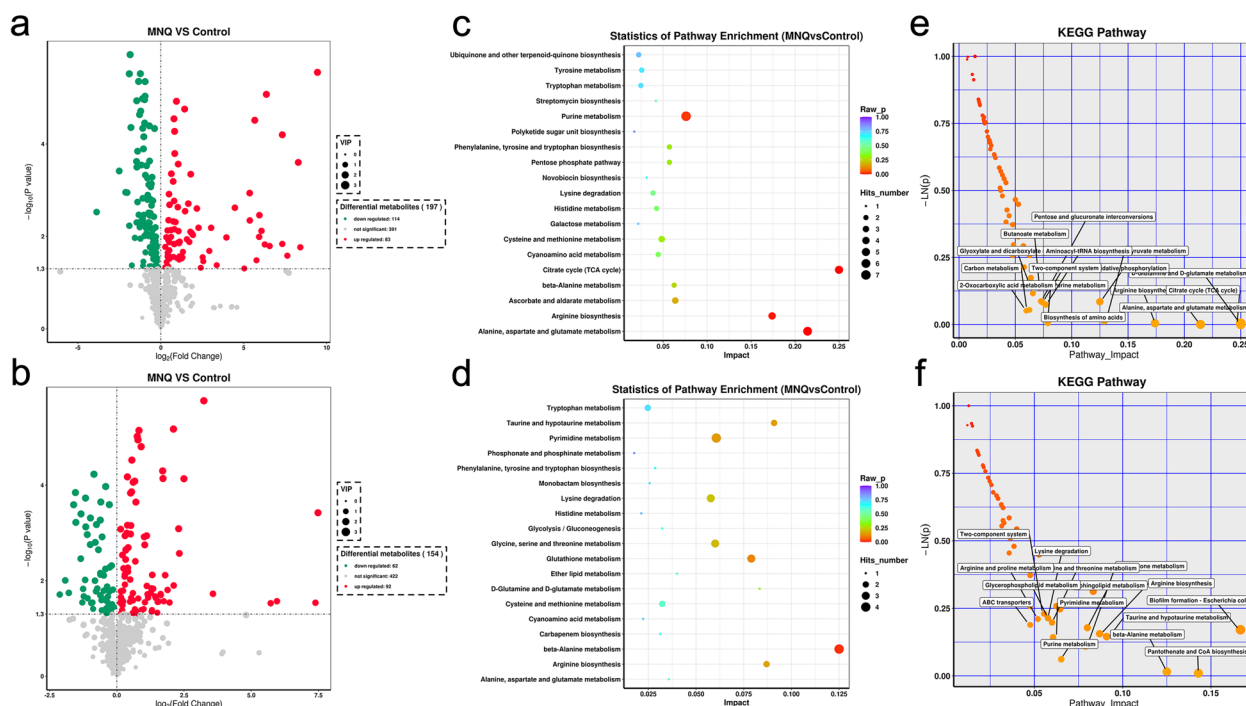


Fig. 7 Multivariate data analysis of bacterial metabolites. Volcano plot for the differentially expressed metabolites under the treatment of MNQ in the NEG mode (a) and POS mode (b). Red circles represent up-regulated metabolites. Green circles represent down-regulated metabolites. Grey circles represent non-significant metabolites. The enriched pathways related to the differential metabolites in the NEG mode (c, e) and POS mode (d, f) by KEGG (Kyoto Encyclopedia of Genes and Genomes) enrichment analysis. The data are representative of six biological replicates

The existing results illustrated that the multiple mechanisms underlying its mode of action involve directly inhibiting Tet(X3)/Tet(X4) catalytic activity and proteins synthesis in *tet(X3)/tet(X4)*-positive pathogens, undermining the functions of PMF-driven efflux pump, and accelerating bacterial metabolic homeostasis imbalance.

MNQ reverses tetracyclines resistance in vivo

To extend clinical application of MNQ, further work is imperative to evaluate the efficacy and cytotoxicity of candidate drugs. Encouragingly, we found that MNQ at the indicated effectively concentrations, or combined with tetracyclines exhibited negligible cytotoxicity in Caco2, HEK-293, and HeLa cells (Supplementary Fig. 6a and b). Additionally, the combination of tetracycline and MNQ (2–128 $\mu\text{g}/\text{mL}$) displayed no significant hemolytic activity to RBCs (Supplementary Fig. 6c). Moreover, for the toxicity test of MNQ, no mortality was observed in 10-day studies. And no treatment-related adverse effects were observed in body weight or adverse biological responses (Supplementary Fig. 6d and e). In addition, safety assessments manifested that compared with the control group, the histopathological examination consisted of hearts, livers, spleens, lungs and kidneys showed no abnormal signs (Supplementary Fig. 6f and g).

These results confirmed satisfactory pharmaceutical properties and safety profile of MNQ with no overt toxicity up to 5 and 15 mg/kg body weight.

Then, the synergistic efficacy of MNQ with tetracyclines in vivo was further evaluated using two mice infection models.

Mouse thigh infection model

A schematic of the combinatorial therapy protocol was shown in Fig. 8a. Compared with the monotherapy, the combination therapy of tetracycline and MNQ (5+5 or 10+5 mg/kg) significantly decreased the bacterial burden in mouse thigh muscle (Fig. 8b). Dramatically, haemorrhage, hyperemia, substantial inflammatory cells infiltration in muscle tissue, abscess formation and tissue necrosis were observed by *E. coli* infection, as evidenced by H&E staining and gross pathological observation (Fig. 8c). Whereas, the combination of MNQ plus tetracycline prominently alleviated thigh abscess lesion (Fig. 8c), indicating that MNQ could potentiate tetracycline activity against *E. coli* 47EC infection.

Systemic infection model in mice

E. coli DH 5 α + pAM401-*tet(X4)*-infected mice systemic infection model was further employed to verify the

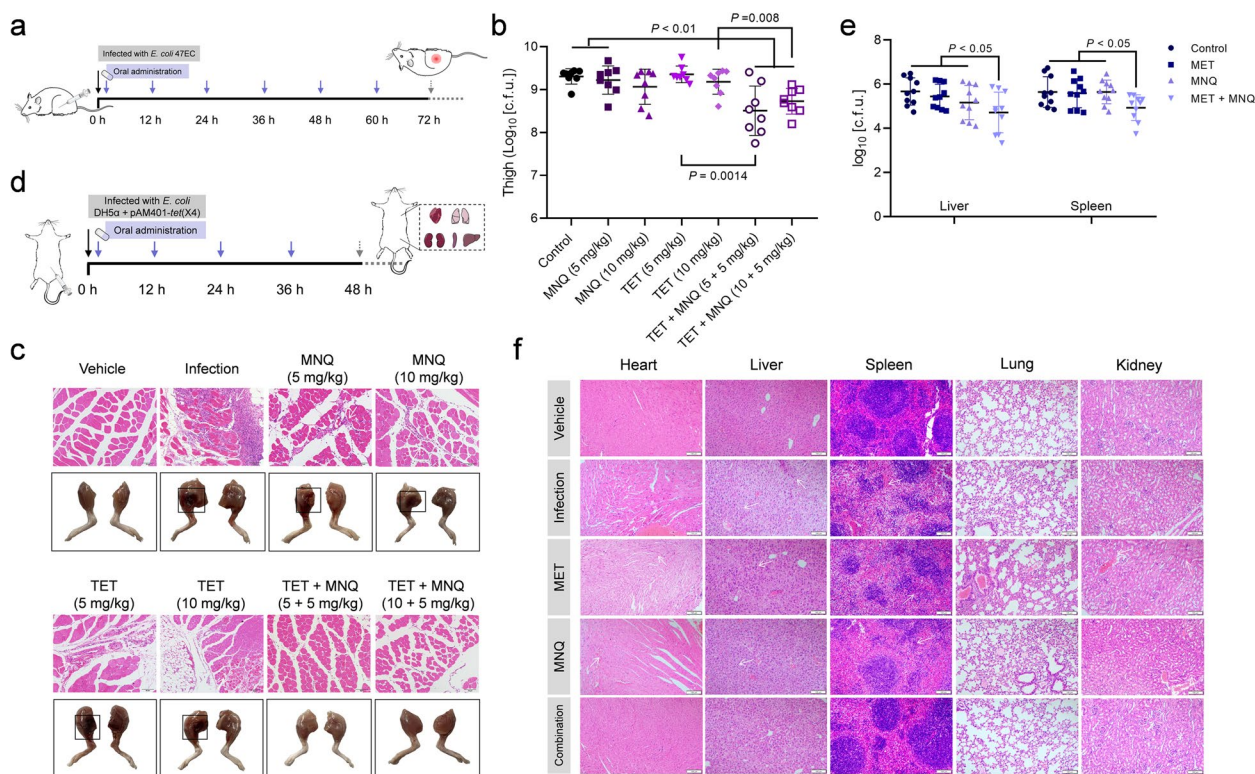


Fig. 8 MNQ rescues tetracyclines activity in vivo. Scheme of the experimental protocols for the thigh infection model induced by *E. coli* 47EC (a) and *E. coli* DH5α + pAM401-tet(X4)-evoked systemic infection model (d). **b** In the mouse thigh infection model, bacterial load in infected thigh muscle were markedly decreased by combination therapy (n = 8 per group). **c** Histopathology and macroscopic observation of the infected thigh muscle. **e** Additionally, in the systemic infection model, the bacterial burden in the livers and spleens of mice challenged with a intraperitoneal inoculation of *E. coli* DH5α + pAM401-tet(X4) (n = 10 per group). **f** H&E staining for the histopathological changes of mice heart, liver, spleen, lung and kidney at 48 h post-infection. And the typical pathological lesions were marked using white arrow

potential of MNQ to enhance the efficacy of methacycline in vivo (Fig. 8d). As shown in Fig. 8e, the bacterial load in livers and spleens were significantly decreased by the combination therapy of methacycline and MNQ, which further confirmed by the alleviated pathological changes (Fig. 8f). Hematoxylin and eosin (H&E) staining of major organs in the *E. coli*-infection mice showed severe morphological damages and fibrosis of myocardial cells, necrosis and congestion in germinal center of spleen, severe cellular degeneration and spotty necrosis in livers, thickened alveolar septum and accumulating inflammatory cell in lungs, renal tubular damage in kidneys. Whereas, pathological damage were obviously alleviated by the combination therapy (Fig. 8f). Collectively, these data convincingly confirmed the adjuvant potential of MNQ with methacycline to tackle MDR bacterial infections.

Discussion

The emergence and evolution of *tet(X)* orthologs paralysed the tetracycline antibiotic therapeutic efficacy and posed a severe threat to public health [8, 9]. Given that

combination approaches potentiate antibiotics activity to address this crisis, we evaluated synergetic activity of quinones with tetracyclines derived from over 200 candidate compounds, and in light of the structural determinants and functional importance of quinones, our findings suggested that the introduction of lipid soluble groups, such as methyl (plumbagin) or substituted methoxyl (2-methoxy-1,4-naphthoquinone) to the 2- position, or chlorine (2,3-dichloro-1,4-naphthoquinone) into the C-2,3 position effectively restored tetracyclines activity against *tet(X3)/tet(X4)*-positive *E. coli*. Remarkably, among the active substances, MNQ with negligible cytotoxicity exhibited the potent potentiation (4 to 32-fold) with tetracyclines against MDR pathogens.

MNQ, a diverse class of 1,4-naphthoquinones, was isolated from *Impatiens glandulifera* and its potential pharmacoeactive and applications have not been extensively explored, especially for the infection therapeutics. In the current study, MNQ as a novel tetracyclines adjuvant significantly potentiates tetracyclines activity. The synergetic mechanisms in *tet(X3)/tet(X4)*-positive pathogens revealed that MNQ potently inhibited the catalytic

activity and production of Tet(X3)/Tet(X4) by engaging with the catalytic pocket of Tet(X3)/Tet(X4). Additionally, exposure to MNQ enhanced membrane permeability and dramatically undermined efflux pump activity. Moreover, MNQ works synergistically with tetracyclines by perturbation of bacterial metabolism homeostasis, which brought about the disturbance of amino acid metabolism and multidrug resistance ATP-binding cassette (ABC) transporters were also perturbed. Inspiredly, understanding how the combination therapy impact bacterial metabolism may provide insight into the concrete mechanisms of action and support evidences to potentiate antibiotics activity may be an effective means [11].

Moreover, we found that MNQ works synergistically with tetracyclines to destroy the biofilms formation and maturation, which provide a promising outlook for the potential application of MNQ as an antibiotic-potentiating adjuvant to treat chronic infection or prevent secondary bacterial infections. Encouragingly, in the two infection models used in our study, MNQ exhibited a robust potentiation with the tested antibiotics against MDR pathogens infections *in vivo*, as evidenced by decreased bacterial counts. Worryingly, poor water solubility and low bioavailability always limited the clinical utility of MNQ. To tackle these problems, improving the dosage form and developing other drivers for effective delivery, for instance, ointments, polymeric microparticles and nanoparticles, were apparently promising, high-efficacy, low-cost and low-toxicity strategies.

In conclusion, we found that MNQ derived from quinones exhibited robust synergistic activities with tetracyclines against MDR pathogens, which provided versatile structural scaffolds for antibiotic adjuvants discovery. Importantly, the discovery of MNQ with distinctive mechanisms highlights great promise for infection therapeutics.

Methods

Reagents

Unless otherwise noted, commercial reagents and solvents were purchased from commercial suppliers and applied without further purification. Purities of all tested compounds were confirmed to be >95% by high-performance liquid chromatography (HPLC) analysis.

Cell lines and cell culture

Human epithelial colon carcinoma (Caco2) cells line, human embryonic kidney (HEK293) cells line and human cervical carcinoma (HeLa) cells line were cultured in high glucose Dulbecco's Modified Eagles Medium (DMEM) with 10% foetal bovine serum (FBS, Biological Industries) and 1% (w:v) penicillin-streptomycin at 37°C. All cell lines were obtained from the American Type Culture Collection (ATCC).

Mice

Female BALB/c mice (6–8 weeks) were purchased from Liaoning Changsheng Technology Industrial Co., Ltd (Liaoning, China). Mice were acclimated in a standardized environment (constant temperature of $23 \pm 2^\circ\text{C}$ and humidity of 55%) for 1 week. All experimental procedures were strictly adhered to the guidelines of the Jilin University Institutional Animal Care Committee.

Antimicrobial susceptibilities

Bacteria used in this study were listed in the Supplementary Table 1. Minimum inhibitory concentrations (MICs) of potential candidate compounds and antibiotics were determined by the broth micro-dilution susceptibility test in Mueller–Hinton broth (MHB, Qingdao Hope Bio-Technology Co., Ltd. (Qingdao, China)), according to the Clinical and Laboratory Standards Institute (CLSI) 2015 guidelines [22]. After 16–24 h incubation at 37°C, MIC values against the bacterial isolates were defined as the lowest concentrations of antimicrobial agents with no visible growth of bacteria.

Synergistic activity of antibiotics and candidate compounds was evaluated by checkerboard assays as described previously [23]. Antibiotics and candidate compounds were serially diluted in a sterile 96-well microtiter plate. After 16–24 h co-incubation with bacterial suspension (5×10^5 CFUs/well), the MIC values of each combination were monitored and then used for FIC index (FICI) calculation according to the following formula [24]: $\text{FIC index} = \text{FICI}_A + \text{FICI}_B = \text{MIC}_{AB} / (\text{MIC}_A + \text{MIC}_{BA}) / \text{MIC}_B$. MIC_A and MIC_B are the MIC of compound A and B, respectively; MIC_{AB} and MIC_{BA} are the MIC of one compound in combination with another. And $\text{FICI} \leq 0.5$ was defined as synergistic.

Time-dependent killing assay

Overnight cultures of *E. coli* DH5 α +pAM401-*tet*(X3) and *E. coli* DH 5 α +pAM401-*tet*(X4) were respectively diluted 1:1000 in MHB medium and incubated at 37°C with shaking at 180 rpm. At the initial exponential phase of growth, different concentrations of MNQ, tetracycline or the combinations were added and incubated for the microbiological plating at the indicated time point. And the colony-forming units (CFUs) were calculated after incubation at 37°C for 24 h.

Resistance development analysis

Sequential culturing of *E. coli* DH5 α +pAM401-*tet*(X3)/*tet*(X4) supplemented with subinhibitory levels of MNQ, TIG, or the combinations was repeated for 25 days. After 24 h co-incubation, the MICs of cultures were determined by broth micro dilutions in 96-well microtiter plates.

Biofilm formation and inhibition assays

Biofilm inhibition assays

Overnight bacterial cultures were diluted to 1×10^6 CFUs/mL with fresh MHB broth in the presence or absence of tetracycline, MNQ or the combinations in a 24-well plate. The formation of biofilms were developed for 24 h at 37°C. Then, the supernatant per well was decanted and the washed biofilm was stained with 0.1% crystal violet (CV). The CV-staining biomass in each well was solubilized with 33% glacial acetic acid and quantified by measuring the absorption values at OD_{570 nm} using a microplate reader (BioTek SLXFA, Winooski, VT, USA).

Biofilm disruption assays

For the biofilm destruction assays, biofilms were initially grown for 12 h in the condition of static cultures at 37°C, as described above. Subsequently, the spent supernatant was removed and the indicated concentrations of tetracycline, MNQ or the combinations (diluted in MHB medium) was supplemented into the wells respectively and incubated for an additional 12 h to analyse the disruption of biofilm via crystal violet (CV) staining.

Confocal microscopy images of biofilms

For the biofilm imaging and analysis, confocal laser scanning microscopy (CLSM) was further employed. Briefly, the biofilm formation and inhibition assays were performed as described above and the media was removed, the underlying biofilms were labeled with SYTO 9 and PI (LIVE/DEAD BacLight Bacterial Viability Kit, Invitrogen, Carlsbad, CA, USA) in the dark environment. The samples were visualized using an inverted confocal laser scanning microscope. And the biofilm thickness of each groups was evaluated using ImageJ software (version number 1.8.0).

Bacterial viability determination

Overnight bacterial cultures were diluted and incubated with tetracycline, MNQ or the combinations for 5 h with the shaking of 200 rpm at 37°C. The bacterial cells were collected, washed and resuspended in PBS. For CLSM observation, the cells (OD_{600 nm} = 0.8) were stained using the LIVE/DEAD BacLight Bacterial Viability Kit (Invitrogen). And the fluorescent intensity was quantified using ImageJ software.

Proton gradient determination

E. coli DH5α + pAM401-*tet*(X4) cultures were washed, collected and resuspended with HEPES (5 mM, pH 7.0) to OD_{600 nm} of 0.5. And the proton motive force was determined using pH-sensitive fluorescence probe BCECF-AM (Merck, Billerica, USA), to recapitulate, the cells

were incubated with BCECF-AM (10 μM) at 37°C for 1 h and incubated with the indicated concentrations of tetracycline, MNQ or the combinations for an additional 1 h. Then, the fluorescent intensity was determined at the excitation and emission wavelengths of 488/535 nm.

Membrane depolarization analysis

Bacterial cultures were washed and resuspended to 5×10^8 CFUs/mL. Then, 3, 3-dipropylthiadicarbocyanine iodide DiSC₃(5) (2 μM; Aladdin, Shanghai, China) was added and measured with excitation wavelength at 622 nm and emission wavelength at 670 nm continuously for 10 min. Whereas, the indicated concentrations of MNQ, tetracycline or the combinations were supplemented and measured for an additional 30 min.

Intracellular ATP analysis

The bacterial lysis supernatant co-incubated with MNQ, tetracycline or the combinations was collected for the determination of Intracellular ATP level, using an Enhanced ATP Assay Kit (Beyotime, Shanghai, China).

Inner membrane (IM) integrity assay

Bacterial cells were washed, resuspended and cultured with MNQ, tetracycline or the combinations for 1 h, followed by the addition of 10 nM propidium iodide (PI; Sigma-Aldrich, St Louis, MO, USA). After incubation for 30 min, membrane integrity was determined by measuring with the excitation wavelength at 535 nm and emission wavelength at 615 nm.

Extracellular β-galactosidase determination

E. coli DH5α + pAM401-*tet*(X4) were washed, collected and resuspended to adjust an OD_{600 nm} of 0.5. After treated with MNQ, tetracycline or the combinations for 1 h at 37°C, the bacterial supernatants were collected and mixed with 3 mM o-nitrophenyl-β-d-galactopyranoside (ONPG; Aladdin) for 2 h at 37°C. Ultimately, the activity of β-galactosidase was determined by measuring at OD_{420 nm} using the microplate reader (BioTek SLXFA, Winooski, VT, USA).

Efflux pump assay

Rhodamine B efflux analysis

To probe whether efflux pump plays a vital role in the recovery of antibacterial activity of tetracyclines plus MNQ, a specific fluorescent dye Rhodamine B (Sigma-Aldrich, St Louis, MO, USA) was applied to analyse the effect of MNQ on the efflux pumps [25]. Bacterial cultures were washed and resuspended to obtain an OD_{600 nm} of 0.5, then cultured with Rhodamine B (5 μM) for 30 min at 37°C. After washing for three times, the bacterial suspension was harvested and co-incubated with

the indicated concentrations of tetracycline, MNQ or the combinations for 1 h, respectively. The fluorescence intensity of bacterial co-culture supernatant was measured at the excitation/emission wavelength at 553 nm/627 nm.

Ethidium bromide (EtBr) efflux assay

To explore the effect of MNQ on the inhibition of multidrug efflux pump, an EtBr efflux assay was performed as described previously [26]. In brief, overnight bacterial culture adjusted to an OD_{600 nm} of 0.5 was cultured with 5 μM EtBr and indicated concentrations of tetracycline, MNQ or the combinations at 37 °C for 1 h. After centrifuged at 5000×g at 4 °C, the bacterial pellets were resuspended with MH-broth. And efflux pump activity was determined using a microplate reader at the excitation/emission wavelength at 526 nm/605 nm.

Recombinant Tet(X3)/Tet(X4) construction, expression and purification

For the production of recombinant pGEX-4 T-1-Tet(X3)/Tet(X4) and the specific mutants, prokaryotic expression systems were employed and performed according to our previous study [13]. And the specific primers used in the current study are listed in Supplementary Table 2.

Enzyme inhibition assay

The purified protein Tet(X3)/Tet(X4) exposed to the indicated concentrations of MNQ in the presence of NADPH, Mg²⁺ and O₂ were incubated at 37 °C for 30 min. Subsequently, the cultures were mixed with tetracycline for an additional 30 min. And the inhibition of catalytic activity was determined by the absorbance at 400 nm and expressed as Inhibition (%) = $(1 - (\Delta OD_{400} \text{ compounds} / \Delta OD_{400} \text{ Vehicle control})) \times 100\%$.

Molecular docking and molecular dynamics (MD) simulations

The PDB code obtained from the Protein Data Bank (PDB) for the crystal structure of Tet(X3)/Tet(X4) was 4A6N. Before docking, a 100-ns molecular dynamics simulation of Tet(X3)/Tet(X4) was performed using AutoDock Vina to establish a Tet(X3)/Tet(X4) crystal structure. Then, the standard docking molecular docking and MD simulations of MNQ-Tet(X3)/Tet(X4) complexes were performed as described previously [13].

The molecular mechanics/Poisson-Boltzmann surface area (MM-PBSA) approach supplied with the Amber 10 package were further employed for the calculation of the interaction energy of MNQ-Tet(X3)/Tet(X4) complexes, including the van der Waals contribution (ΔE_{vdw}), the electrostatic contribution (ΔE_{ele}) and the solvation contribution (ΔE_{sol}) and the total contribution (ΔE_{total}) [27, 28].

Circular dichroism (CD) spectroscopy

Tet(X3)/Tet(X4) in the presence of MNQ (128 μg/mL) or DMSO was prepared and CD spectroscopy was employed to explore the effects of MNQ on the Tet(X3)/Tet(X4) secondary structure. Briefly, CD spectra with the scanning wavelengths ranged from 190 to 250 nm at a 0.5 nm interval were recorded using a CD spectrometer and analysed via the BeStSel web server (<https://bestsel.elte.hu/index.php>).

Fluorescence quenching assay

Fluorescence quenching was employed to investigate the interaction of MNQ with the proteins. Briefly, the equilibrium binding constants for MNQ with Tet(X3)-WT, Tet(X3)-L222A, Tet(X3)-M215A, Tet(X3)-F224A, or Tet(X4)-WT, Tet(X4)-L219A, Tet(X4)-I234A were examined at the excitation/emission wavelength of 280 nm/345 nm.

Western blotting analysis

Western blotting assay was employed to explore the effect of MNQ on the production of Tet(X3)/Tet(X4). Tet(X3)/Tet(X4)-positive bacteria co-incubated with different concentrations of MNQ (0, 16, 32, 64 μg/mL) were collected to analyze the expression of Tet(X3)/Tet(X4). Briefly, the samples were separated on 10% SDS-PAGE gels, and transferred to polyvinylidene difluoride (PVDF) membranes. After blocking with 5% (w/v) skimmed milk for 2 h, the membranes were incubated with the indicated primary antibodies at room temperature for 2 h and HRP-conjugated goat anti-mouse secondary antibodies for an additional 2 h. The blots were visualized using an enhanced chemiluminescence ECL kit (Biosharp, Beijing, China).

Quantitative reverse transcription-PCR (qRT-PCR) analysis

Overnight *E. coli* DH5α + pAM401-*tet(X3)/tet(X4)* were further cultured with or without MNQ and total bacterial RNA was extracted using TRIzol (TransGen Biotech, Beijing, China) according to previous report [29]. Then, 1000 ng extracted RNA was reverse-transcribed using NovoScript[®] Plus All-in-one 1st Strand cDNA Synthesis SuperMix (gDNA Purge) (catalogue no. E047-01B; Novoprotein, Suzhou, China) following the manufacturer's protocol. The mRNA levels of *tet(X3)/tet(X4)* in *E. coli* were performed with NovoScript[®] SYBR qPCR SuperMix Plus (catalogue no. E096-01B; Novoprotein). PCR procedures were described previously [12]. And 16S rRNA was served as an endogenous control.

Metabolomic analysis

Bacterial culture of *E. coli* DH 5α + pAM401-*tet(X4)* in the presence or absence of MNQ (128 μg/mL) was

prepared for subsequent experiments. Bacterial samples were analysed based on the Ultra High Performance Liquid Chromatography Q Exactive Mass Spectrometer (UHPLC-QE-MS, Thermo, Waltham, MA, USA) following the procedures described previously [30]. The ionization source of LC-MS is electrospray ionization and both positive ion (POS) mode and negative ion (NEG) mode were employed to achieve maximal coverage for bacterial metabolites. Briefly, MS raw data involving the peak number, sample name and normalized peak area were processed with R package metaX and analysed for principal component analysis (PCA) and orthogonal partial least square-discriminate analysis (OPLS-DA). PCA indicated the distribution of origin data. Additionally, supervised OPLS-DA was further applied to detail group separation and facilitate classification. The results of screening differential metabolites were visualized using a volcano plot. By means of the Kyoto Encyclopedia of Genes and Genomes (KEGG, <http://www.kegg.jp>) [31] and MetaboAnalyst (<http://www.metaboanalyst.ca/>) [32], we further explored the key metabolic pathways represented by the differential metabolites and analysed the biological functional alterations.

In vitro cytotoxicity evaluation

Fresh washed rabbit erythrocytes in the presence or absence of MNQ, or the combination of MNQ and tetracycline were incubated at 37°C for 1 h. And the culture supernates were harvested and measured at OD_{570 nm} using a microplate reader (BioTek SLXFA).

Additionally, Caco2 cells, HeLa cells and HEK-293 cells were incubated with the indicated concentrations of MNQ, either alone or in combination with tetracyclines for 5 h and the cell viability was detected by a Cytotoxicity Detection Kit (Roche, Basel, Switzerland) according to the manufacturer's instructions.

Animal study

In vivo-toxicity evaluation

To evaluate the toxic effects of MNQ *in vivo*, BALB/c mice (6–8 weeks, $n=6$ per group) were orally administered with MNQ at 5 or 15 mg/kg body weight at 12-h intervals for continuously 5 days. The clinical characterizations including animal behaviors and body weight were observed and monitored daily for 10 days. At experimental end points, all mice were euthanized, followed by the histological observation of tissues and organs, then fixed in 4% formaldehyde and stained with haematoxylin and eosin (H&E) for pathological analysis.

Mice thigh infection model

Given that tetracyclines [33] and quinones [34, 35] exhibited the similar pharmacokinetic parameters, such as the

terminal elimination half-life ($t_{1/2}$) and time to maximal drug concentration (t_{max}) in the previous study, combination regimens to maximize the synergistic antibacterial activity *in vivo* were employed in the current study.

E. coli 47EC (1.0×10^8 CFU) was injected into the left thigh muscle of mice, which caused localized bacterial infection and abscess formation. MNQ (resuspended in 0.5% CMC-Na, 5 mg/kg or 10 mg/kg), tetracycline (TET, dissolved in water, 5 mg/kg or 10 mg/kg), and the combinations was administered intragastrically in the indicated concentrations, respectively. The vehicle-treated group received the equal amount of solvent control (0.5% CMC-Na) by oral administration. At 72 h post-infection, the infected thigh muscles of mice were homogenized, diluted and plated on MHB agar plates for CFU counting. Further, the infected muscles in each groups were fixed and preserved in 4% formaldehyde for pathological observation using haematoxylin and eosin (H&E) staining.

Mice systemic infection model

Exponentially growing *E. coli* DH5 α +pAM401-*tet*(X4) was collected and adjusted to 1.0×10^8 CFU. All mice were infected by intraperitoneal injection of bacterial cultures. And the mice were randomly divided into 4 groups: *E. coli* infection group, 5 mg/kg MNQ (resuspended in 0.5% CMC-Na) treatment, 10 mg/kg methacycline (MET, dissolved in water) treatment, combined therapy of MNQ+MET (5 mg/kg+10 mg/kg). The therapeutic doses selection for *E. coli* DH5 α +pAM401-*tet*(X4) systemic infection were referred by the thigh infection model described above. All the drugs were orally administrated at 12-h intervals, and at 48 h post-infection, all mice were euthanised for the histopathological lesion assessment. Briefly, the histopathological changes in the hearts, livers, spleens, lungs and kidneys in each group were assessed using H&E staining for observation. Additionally, livers and spleens were collected, homogenized and diluted with sterilized PBS for microbiological plating to evaluate the bacterial burdens.

Statistical analysis

Statistical analysis was performed using GraphPad Prism 8.0 software. All data are expressed as the means \pm SEM. Sample size (n) was mentioned in the figure legends and the statistical significance was analyzed by the unpaired student's *t*-test method between two groups or one-way ANOVA (analysis of variance) among multiple groups to calculate *P* values ($*P < 0.05$; $**P < 0.01$; ns, $P \geq 0.05$). Differences with $P < 0.05$ were regarded as significant.

Supplementary Information

The online version contains supplementary material available at <https://doi.org/10.1186/s44280-023-00030-y>.

Additional file 1: Supplementary Fig. 1. MNQ potentiates tetracyclines activity. **Supplementary Fig. 2.** MNQ is an available broad-spectrum synergist. **Supplementary Fig. 3.** Disruption of bacterial biofilms by combination treatment. **Supplementary Fig. 4.** MNQ addition triggers cellular membrane damage. **Supplementary Fig. 5.** Two multivariate exploratory analyses were performed to evaluate separation between control and MNQ treatment group. **Supplementary Fig. 6.** Safety evaluations of MNQ *in vivo/in vitro*. **Supplementary Table 1.** The bacterial strains used in the current study. **Supplementary Table 2.** Sequence of primers used for protein purification and site-directed mutagenesis. **Supplementary Table 3.** Synergistic activities of tetracycline antibiotics (tetracycline/tigecycline) and quinones combination therapy against *E. coli* DH 5α + pAM401-*tet*(X4). **Supplementary Table 4.** Antimicrobial susceptibility test of MNQ combined with tetracycline against *tet*(X4)/*tet*(X6)-positive isolates. **Supplementary Table 5.** Antimicrobial susceptibility test of MNQ combined with tigecycline against *tet*(X4)-positive isolates of chicken origin.

Acknowledgements

Part of the material was modified from Servier Medical Art (<http://smart.servier.com/>), licensed under a Creative Common Attribution 3.0 Unported License. This work was supported by the National Natural Science Foundation of China (grant No. U22A20523, 32202856, 32172912 and 32102723), the Post-doctoral Research Foundation of China (Certificate Number: 2023 M731291), Interdisciplinary Integration and Innovation Project of JLU (JLUXKJC2021QZ04) and the Graduate Innovation Fund of Jilin University (No. 2022001). All authors report no potential conflicts.

Authors' contributions

L.X., Y.Z., H.F., X.D., D.L. and J.W. conceived and designed this project. L.X., Y.Z., H.S., N.X., X.N., D.O., H.Y., M.S. and P.Z. performed experiments; L.X. and Y.Z. analyzed the data and prepared figures; L.X., Y.Z. and J.W. drafted the manuscript. J.W., D.L., H.F. and X.D. accessed and verified the underlying data. All authors have read, reviewed and approved the final manuscript.

Availability of data and materials

The data are available from the corresponding author upon reasonable request.

Declarations

Ethics approval and consent to participate

All experiments protocols and procedures were strictly adhered to the guidelines of the Jilin University Institutional Animal Care Committee (approval no. ALKT202012006).

Competing interests

No potential conflict of interest was reported by the authors.

Received: 15 August 2023 Revised: 6 November 2023 Accepted: 17 November 2023

Published online: 10 January 2024

References

- Thakare R, Kesharwani P, Dasgupta A, Srinivas N, Chopra S. Antibiotics: past, present, and future. *Curr Opin Microbiol*. 2019;51:72–80. <https://doi.org/10.1016/j.mib.2019.10.008>.
- Board E. Antimicrobial resistance: a threat to global health security. World Health Organization. 2005.
- Yan Y-H, Li G, Li G-B. Principles and current strategies targeting metallo-β-lactamase mediated antibacterial resistance. *Med Res Rev*. 2020;40(5):1558–92.
- Liu YY, Wang Y, Walsh TR, Yi LX, Zhang R, Spencer J, et al. Emergence of plasmid-mediated colistin resistance mechanism MCR-1 in animals and human beings in China: a microbiological and molecular biological study. *Lancet*. 2015;16(2):161–8.
- Nguyen F, Starosta AL, Arenz S, Sohmen D, Dönhöfer A, Wilson DN. Tetracycline antibiotics and resistance mechanisms. *Biol Chem*. 2014;395(5):559–75.
- Grossman TH. Tetracycline antibiotics and resistance. *Cold Spring Harb Perspect Med*. 2016;6(4):a025387.
- Sun J, Chen C, Cui CY, Zhang Y, Liu X, Cui ZH, et al. Plasmid-encoded *tet*(X) genes that confer high-level tigecycline resistance in *Escherichia coli*. *Nat Microbiol*. 2019;4(9):1457–64.
- He T, Wang R, Liu DJ, Walsh TR, Zhang R, Lv Y, et al. Emergence of plasmid-mediated high-level tigecycline resistance genes in animals and humans. *Nat Microbiol*. 2019;4(9):1450–6.
- Fang LX, Chen C, Cui CY, Li XP, Zhang Y, Liao XP, et al. Emerging high-level Tigecycline resistance: novel tetracycline destructases spread via the Mobile Tet(X). *Bioessays*. 2020;42(8):e2000014.
- Lee BS, Kalia NP, Jin XEF, Hasenoehrl EJ, Berney M, Pethe K. Inhibitors of energy metabolism interfere with antibiotic-induced death in *Mycobacterium*. *J Biol Chem*. 2019;294(6):1936–43.
- Kohanski MA, Dwyer DJ, Hayete B, Lawrence CA, Collins JJ. A common mechanism of cellular death induced by bactericidal antibiotics. *Cell*. 2007;130(5):797–810.
- Song MR, Liu Y, Huang XY, Ding SY, Wang Y, Shen JZ, et al. A broad-spectrum antibiotic adjuvant reverses multidrug-resistant gram-negative pathogens. *Nat Microbiol*. 2020;5(8):1040–50.
- Xu L, Zhou YL, Niu S, Liu ZY, Zou YN, Yang YA, et al. A novel inhibitor of monooxygenase reversed the activity of tetracyclines against *tet*(X3)/*tet*(X4)-positive bacteria. *Ebiomedicine*. 2022;78:103943.
- Patel OPS, Beteck RM, Legoabe LJ. Antimalarial application of quinones: a recent update. *Eur J Med Chem*. 2021;210:113084.
- Ahn JH, Cho SY, Ha JD, Chu SY, Jung SH, Jung YS, et al. Synthesis and PTP1B inhibition of 1,2-naphthoquinone derivatives as potent anti-diabetic agents. *Bioorg Med Chem Lett*. 2002;12(15):1941–6.
- Milackova I, Prnova MS, Majekova M, Sotnikova R, Stasko M, Kovacicova L, et al. 2-Chloro-1,4-naphthoquinone derivative of quercetin as an inhibitor of aldose reductase and anti-inflammatory agent. *J Enzyme Inhib Med Chem*. 2015;30(1):107–13.
- Ravichandiran P, Maslyk M, Sheet S, Janeczko M, Premnath D, Kim AR, et al. Synthesis and antimicrobial evaluation of 1,4-naphthoquinone derivatives as potential antibacterial agents. *ChemistryOpen*. 2019;8(5):589–600.
- Vuotto C, Donelli G. Novel treatment strategies for biofilm-based infections. *Drugs*. 2019;79(15):1635–55.
- Yang WR, Moore IF, Koteva KP, Bareich DC, Hughes DW, Wright GD. TetX is a flavin-dependent monooxygenase conferring resistance to tetracycline antibiotics. *J Biol Chem*. 2004;279(50):52346–52.
- Hurtado-Rios JJ, Carrasco-Navarro U, Almanza-Pérez JC, Ponce-Alquicira E. Ribosomes: the new role of ribosomal proteins as natural antimicrobials. *Int J Mol Sci*. 2022;23(16):9123.
- Le D, Krasnopeeva E, Sinjab F, Pilizota T, Kim M. Active efflux leads to heterogeneous dissipation of proton motive force by Protonophores in Bacteria. *mBio*. 2021;12(4):e0067621.
- CLSI. Performance standards for antimicrobial susceptibility testing. Berwyn: Clinical and Laboratory Standards Institute; 2015.
- Zhou YL, Wang JF, Guo Y, Liu XQ, Liu SL, Niu XD, et al. Discovery of a potential MCR-1 inhibitor that reverses polymyxin activity against clinical *mcr-1*-positive *Enterobacteriaceae*. *J Inf Secur*. 2019;78(5):364–72.
- Macnair CR, Stokes JM, Carfrae LA, Fiebig-Comyn AA, Coombes BK, Mulvey MR, et al. Overcoming *mcr-1* mediated colistin resistance with colistin in combination with other antibiotics. *Nat Commun*. 2018;9(1):458.
- Forster S, Thumser AE, Hood SR, Plant N. Characterization of Rhodamine-123 as a tracer dye for use in *in vitro* drug transport assays. *PLoS One*. 2012;7(3):e33253.
- Kaatz GW, Seo SM, O'Brien L, Wahiduzzaman M, Foster TJ. Evidence for the existence of a multidrug efflux transporter distinct from NorA in *Staphylococcus aureus*. *Antimicrob Agents Chemother*. 2000;44(5):1404–6.
- Schaffner-Barbero C, Gil-Redondo R, Ruiz-Avila LB, Huecas S, Läppchen T, den Blaauwen T, et al. Insights into nucleotide recognition by cell division protein FtsZ from a *mant*-GTP competition assay and molecular dynamics. *Biochemistry*. 2010;49(49):10458–72.

28. Punkvang A, Saparpakorn P, Hannongbua S, Wolschann P, Beyer A, Pungpo P. Investigating the structural basis of arylamides to improve potency against *M. Tuberculosis* strain through molecular dynamics simulations. *Eur J Med Chem*. 2010;45(12):5585–93.
29. Rio DC, Ares M, Hannon GJ, Nielsen TW. Purification of RNA using TRIzol (TRI reagent). *Cold Spring Harb Protoc*. 2010;2010(6):pdb.prot5439.
30. Liu PR, Hu DH, Yuan LL, Lian ZM, Yao XH, Zhu ZB, et al. Metabolomics analysis of PK-15 cells with pseudorabies virus infection based on UHPLC-QE-MS. *Viruses-Basel*. 2022;14(6):1158.
31. Kanehisa M, Goto S. KEGG: Kyoto encyclopedia of genes and genomes. *Nucleic Acids Res*. 2000;28(1):27–30.
32. Xia J, Wishart DS. Using MetaboAnalyst 3.0 for comprehensive metabolomics data analysis. *Curr Protoc Bioinformatics*. 2016;55:14.10(11-91).
33. Agwuh KN, MacGowan A. Pharmacokinetics and pharmacodynamics of the tetracyclines including glycylicyclines. *J Antimicrob Chemother*. 2006;58(2):256–65.
34. Sun Z, Zhao LS, Zuo LH, Qi C, Zhao P, Hou XH. A UHPLC-MS/MS method for simultaneous determination of six flavonoids, gallic acid and 5,8-dihydroxy-1,4-naphthoquinone in rat plasma and its application to a pharmacokinetic study of cortex *Juglandis Mandshuricae* extract. *J Chromatogr B*. 2014;958:55–62.
35. Zhang ZQ, Bai J, Zeng YW, Cai MR, Yao Y, Wu HM, et al. Pharmacology, toxicity and pharmacokinetics of acetylshikonin: a review. *Pharm Biol*. 2020;58(1):950–8.

Publisher's Note

Springer Nature remains neutral with regard to jurisdictional claims in published maps and institutional affiliations.

Ready to submit your research? Choose BMC and benefit from:

- fast, convenient online submission
- thorough peer review by experienced researchers in your field
- rapid publication on acceptance
- support for research data, including large and complex data types
- gold Open Access which fosters wider collaboration and increased citations
- maximum visibility for your research: over 100M website views per year

At BMC, research is always in progress.

Learn more biomedcentral.com/submissions

